T. Magn. Soc. Jpn. (Special Issues)., **2**, 48-51 (2018)

<Paper>

Dependence of thickness of Fe buffer layer on magnetic properties for $Mn_{2.6}Ga$ thin films

K. Sato, Y. Takahashi, H. Makuta, T. Shima and M. Doi

Graduate School of Engineering, Tohoku Gakuin University, Tagajo 980-8573, Japan

$D0_{22}$-$Mn_{2.6}Ga$ thin films were fabricated by an ultra-high vacuum electron beam vapor deposition system on a MgO (100) single crystalline substrate with different buffer layer thicknesses (0.7 - 5 nm). As the annealing temperature T_a increased to 400°C, the squareness of the *M-H* curves improved, and the saturation magnetization M_s and magnetic anisotropy K_u increased. At that time, from XRD patterns, $D0_{22}$-Mn_3Ga (002) superlattice and (004) fundamental peaks were clearly observed from all samples. Our results suggest the existence of a magnetic dead layer of about 3.5 nm in the MnGa layer. Because of this magnetic dead layer, a relatively high K_u of 9.3 Merg/cm^3 and low surface roughness R_a of 0.93 nm were obtained from $Mn_{2.6}Ga$ thin film on a 2-nm Fe buffer at T_a = 400°C. The results in this work suggest that Fe is a suitable buffer layer for perpendicular magnetized $D0_{22}$-MnGa thin film.

Key words: $D0_{22}$-MnGa thin film, saturation magnetization, magnetic anisotropy, electron beam vapor deposition system, surface roughness, buffer layer

1. Introduction

MnGa alloys show $D0_{22}$ and $L1_0$ structure in the composition range at approximately 69 - 76 (η phase) and, 64 - 67 (γ_1 phase) and 58 - 61 (γ_2 phase) at.% Mn in the binary phase diagram[1]. Owning to outstanding magnetic properties such as a high magnetic anisotropy K_u ~ 10 - 23.5 Merg/cm^3 [2-4], a low Gilbert damping constant α ~ 0.008 - 0.015[5], a relatively low saturation magnetization M_s ~ 600 emu/cm^3 [2-4] and a high spin polarization P ~ 58% (experimentally) [5], the MnGa thin films have been studied for applications of spintronic devices, including a magnetic random access memory operated by spin transfer torque (STT-MRAM). This device requires a guarantee of thermal stability and high speed writing and reading. That is to say, STT-MRAM needs perpendicularly magnetized magnetic tunnel junctions (p-MTJs) that have high K_u and P. Nowadays, MTJ is demanded to achieve a high K_u ≧ 10 Merg/cm^3, a high P ≧ 70%, a low α ≦ 0.01 and a low M_s ~ 100 emu/cm^3 [6,7]. From the point of view, a great potentiality for magnetic layers of MTJ is derived from MnGa thin films which shows high K_u, high P, low α and relatively small M_s [8-13]. However, there have been few reports about buffer layers for growth of MnGa thin films. Therefore, it is necessary to obtain the knowledge of buffer layers' dependence on magnetic properties. The lattice mismatch between $D0_{22}$-Mn_3Ga and Fe is smaller than that of $D0_{22}$-Mn_3Ga and Cr. However, it is well known that Fe behaves an in-plane easy magnetization axis. On the other hand, a large perpendicular magnetic anisotropy (PMA) of 14 Merg/cm^3 from ultrathin Fe/MgO interface has been presented by J. W. Koo et al.[14]. The, in-plane easy magnetization axis and the relatively high average roughness R_a of 2.63 nm were observed from MnGa thin films on 5-nm Fe buffer at our previous work[15]. Improvements of these properties are indispensable for application of MTJ films.

In this work, dependence of thickness of Fe buffer layers on magnetic properties for $Mn_{2.6}Ga$ thin films have been investigated by using an ultra-high vacuum electron beam (UHV-EB) vapor deposition system.

2. Experimental procedure

All the samples prepared in this work were grown by an ultra-high vacuum electron beam vapor deposition system with base pressure less than 8.9×10^{-7} Pa. MnGa target was fabricated from row materials of Mn (5N) and Ga (6N), through the arc melting method in argon atmosphere with base pressure less than 10^{-3} Pa. The stacking structure is the MgO (100) single crystalline substrate / the Fe buffer layers (0.7 - 5 nm) / $Mn_{2.6}Ga$ (20 nm) / the Cr capping layer (10 nm). The MgO (100) single crystal substrate was thermally flushed up to 700°C in the UHV chamber half an hour. The Fe buffer layers and the MnGa layer were deposited at room temperature and 300°C, respectively. Finally, the Cr capping layer was deposited at room temperature. Annealing process was carried out at 300 - 500°C 3 hours to improve the crystal quality. All growths are monitored in real time by using reflection high-energy electron diffraction (RHEED). The compositions of the films and the crystal structure of the samples were determined by an energy dispersive X-ray spectroscopy (EDX) and X-ray diffraction (XRD) with Cu-$K\alpha$ radiation, respectively. The surface roughness of film was investigated by atomic force microscopy (AFM). The magnetic properties of thin films were measured by using superconducting quantum interference device (SQUID).

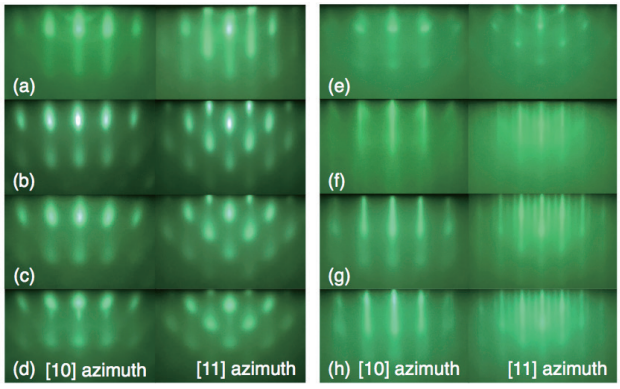

Fig. 1 RHEED patterns for different Fe buffer layer thicknesses and $Mn_{2.6}Ga$ thin films. Fe buffer: (a) 5 nm, (b) 2 nm, (c) 1 nm and (d) 0.7 nm. $Mn_{2.6}Ga$ thin film on Fe buffer: (e) 5 nm, (f) 2 nm, (g) 1 nm and (h) 0.7 nm.

3. Results and discussion

Figure 1 shows RHEED patterns for different Fe buffer layer thickness ((a)-(d)) and $Mn_{2.6}Ga$ thin films on Fe buffer: (e) 5 nm, (f) 2 nm, (g) 1 nm and (h) 0.7 nm, respectively. As the thickness of Fe decreases, RHEED patterns of Fe (From (a) to (d)) became spotty. The result suggested that Fe do not grow layer by layer (Frank-van der Merwe) but island growth (Vol-mer-Weber). Therefore, as Fe becomes thinner, surface roughness of Fe becomes worse. The epitaxial growth of $Mn_{2.6}Ga$ and surface reconstruction structure were observed from (e).

Figure 2 shows XRD patterns for $Mn_{2.6}Ga$ thin films on Fe buffer: (a) 5 nm, (b) 2 nm, (c) 1 nm and (d) 0.7 nm. $D0_{22}$-Mn_3Ga (002) superlattice and (004) fundamental peaks were observed from all samples. Although the broad peaks are shown in (a) and (b), this might be because of the diffusion of Fe. The (004) peak sifted to low angle side, which showed the c-axis became long. The highest ordering parameter $S_{002} = 0.69$ was obtained from (b) 2-nm Fe buffer.

Figure 3 shows magnetization curves for $Mn_{2.6}Ga$ on Fe buffer: (a) 5 nm, (b) 2 nm, (c) 1 nm and (d) 0.7 nm. The black and red lines indicate the out-of-plane and in-plane magnetization curves. The volume of magnetic layer was calculated by combining the thickness of Fe and MnGa. K_u is given by the equation $K_u^{eff} + 2\pi M_s^2$ where K_u^{eff} is the effective perpendicular magnetic anisotropy (PMA) constant. The computation for the determination of K_u^{eff} was carried out in subtracting the area from H_k^{eff} to 0 in the in-plane magnetization curves from the out-of-plane magnetization curves. Here, the effective anisotropy field (H_k^{eff}) was defined as the extrapolated intersection of in-plane magnetization curves with the value of saturation magnetization of out-of-plane magnetization curves. Fig. 3 shows that in the case of (a), the easy magnetization axis is the in-plane direction and (b)-(d) are out-of-plane directions. The result of (a) 5-nm Fe buffer, which shows the easy axis to the in-plane direction, was considered due to

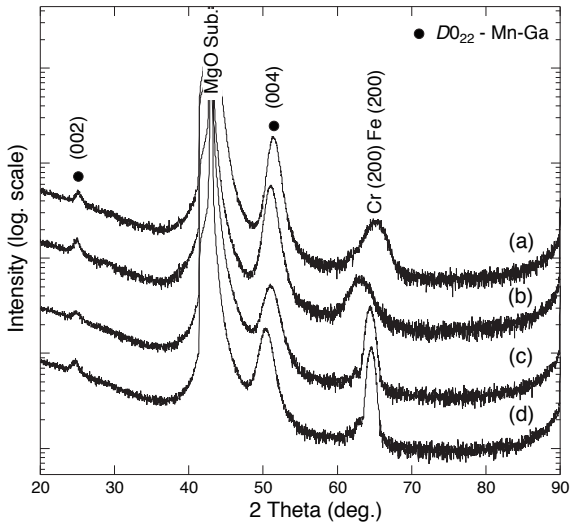

Fig. 2 XRD patterns for $Mn_{2.6}Ga$ thin film on Fe buffer: (a) 5 nm, (b) 2 nm, (c) 1 nm and (d) 0.7 nm.

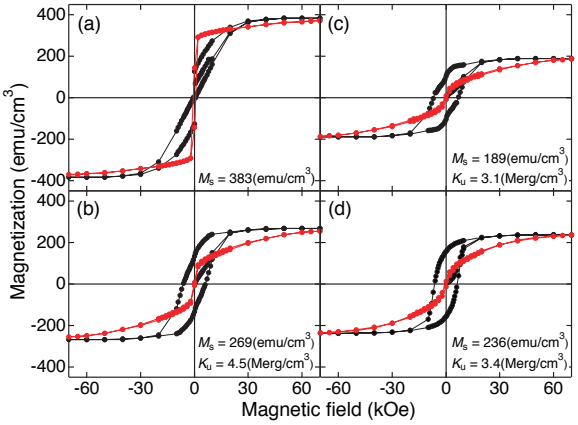

Fig. 3 Magnetization curves for $Mn_{2.6}Ga$ thin film on Fe buffer: (a) 5 nm, (b) 2 nm, (c) 1nm and (d) 0.7 nm. Black and red lines indicate out-of-plane and in-plane magnetization curves.

interface roughness for Fe layer (Neel "orange-peel" coupling though the magnetic dead layer[16,17]). The highest K_u of 4.5 Merg/cm^3 was observed for (b) 2-nm Fe buffer.

Figure 4 shows the product of M_s and t as a function of t. Here, t is a thickness of MnGa layers and M_s is estimated by subtracting magnetization of Fe from total magnetization. The black circles and squares indicate the reference values of $Mn_{1.5}Ga$ thin films on 5-nm Cr buffer presented by Y. Takahashi et al[3], and $Mn_{2.6}Ga$ thin films on 2-nm Fe buffer in this work, respectively. A magnetic dead layer thickness ~ 2 nm in the Cr buffer case and ~ 3.5 nm in the Fe buffer case were shown in Fig. 4. Here, the magnetic dead layer means a layer of non-magnetic ones. It was shown that when Fe used for the buffer layer, the magnetic dead layer becomes larger than in the case of

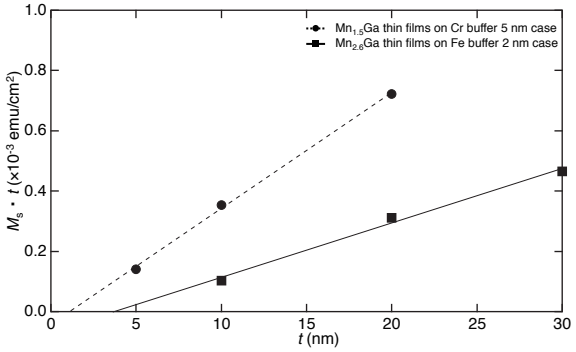

Fig. 4 Product of M_s and t as a function of t. Black circle and square indicate reference value of $Mn_{1.5}Ga$ thin films on 5-nm Cr buffer[3] and $Mn_{2.6}Ga$ thin films on 2-nm Fe buffer in this study, respectively.

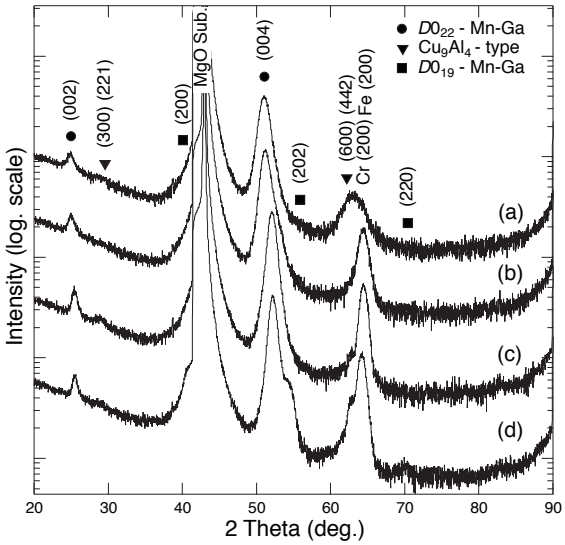

Fig. 5 XRD patterns for $Mn_{2.6}Ga$ on 2-nm Fe buffer (a) without annealing and at (b) T_a = 300°C, (c) 400°C and (d) 500°C.

Cr buffer layers. This result suggest that mixing of MnGa with Fe between their interfaces gives rise to the non-magnetic dead layer. The magnetization is decreased at the mixed layer, which agrees with our previous research that shows the drastic decrease of magnetization by adding Fe into MnGa alloys[18].

Figure 5 shows XRD patterns for $Mn_{2.6}Ga$ on the 2-nm Fe buffer (a) without annealing and at (b) T_a = 300°C, (c) 400°C and (d) 500°C. $D0_{22}$-Mn_3Ga (002) superlattice and (004) fundamental peaks were clearly observed from the all samples. As the T_a increased to (c) from (a), the (004) peak was shifted to a high angle side, which suggest that the c-axis turns to short. In addition, the ordering parameter (S_{002}) increased from 0.69 (a) to 0.78 (c). These results lead to a conclusion that annealing process was effective for the improvement of the crystal quality under T_a = 400°C.

Figure 6 shows magnetization curves for $Mn_{2.6}Ga$ on the 2-nm Fe buffer (a) without annealing and at (b) T_a = 300°C, (c) 400°C and (d) 500°C. As the T_a increased from

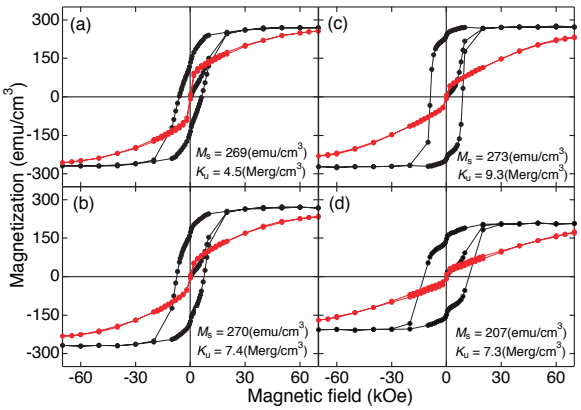

Fig. 6 Magnetization curves for $Mn_{2.6}Ga$ on 2-nm Fe buffer (a) without annealing and at (b) T_a = 300°C, (c) 400°C and (d) 500°C. Black and red lines indicate the out-of-plane and in-plane magnetization curves.

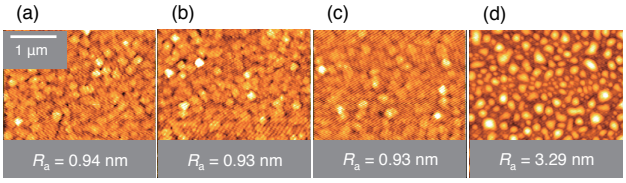

Fig. 7 AFM images for $Mn_{2.6}Ga$ on 2-nm Fe buffer (a) without annealing and at (b) T_a = 300°C, (c) 400°C and (d) 500°C.

(a) to (c), the squareness of the M-H curves improved, and value of both M_s and K_u increased. These values, however, decreased at (d). This result is in good agreement with the result of Fig. 5. The highest M_s of 273 emu/cm^3 and K_u of 9.3 Merg/cm^3 were obtained at (c).

Figure 7 shows AFM images for $Mn_{2.6}Ga$ on the 2-nm Fe buffer (a) without annealing and at (b) T_a = 300°C, (c) 400°C and (d) 500°C. The relatively low surface roughness R_a of 0.93 nm was observed from (b) and (c). In the case of T_a = 500°C, R_a became worse.

4. Summary

In this work, dependence of thickness of Fe buffer layers on magnetic properties for $Mn_{2.6}Ga$ thin films have been investigated by using an ultra-high vacuum electron beam (UHV-EB) vapor deposition system. The highest K_u was obtained from the 2-nm Fe buffer. When T_a is increased to 400°C, improvement of squareness of the M-H curve and increase of M_s and K_u were observed. From the XRD patterns, $D0_{22}$-Mn_3Ga the (002) superlattice and the (004) fundamental peaks were clearly observed from the all samples. Our result indicates that Fe buffer layers made about 3.5 nm of the magnetic dead layers in MnGa. Because of the existence of about 3.5 nm of magnetic dead layer, the relatively high K_u of 9.3 Merg/cm^3 and the low surface roughness R_a of 0.93 nm might be obtained from $Mn_{2.6}Ga$ thin film

on 2-nm Fe buffer at T_a = 400°C. The results in this work suggest that Fe is a suitable buffer layer for application of high K_u $D0_{22}$-MnGa.

Acknowledgements This work was supported in part by the Ministry of Education, Culture, Sports, Science and Technology project for the "Hi-tech Research Center of Tohoku Gakuin University and Grants-in-aid for Scientific Research. Part of this work was supported by "Collaborative Research Based on Industrial Demand" program from Japan Science and technology Agency.

References

1) K. Minakuchi, R. Y. Uematsu, K. Ishida, and, R. Kainuma: *J. Alloy.* Compod., **537**, 332 (2012).
2) S. Mizukami, T. Kubota, F. Wu, X. Zhang, T. Miyazaki, H. Naganuma, M. Oogane, A. Sakuma and Y. Ando: *Phys. Rev.* **B**, 85, 014416 (2012).
3) Y. Takahashi, H. Makuta, T. Shima and M. Doi: *T. Magn. Soc. Jpn. (Special Issues).*, **1**, 30-33 (2017).
4) H. Makuta, Y. Takahashi, T. Shima and M. Doi: *T. Magn. Soc. Jpn. (Special Issues).*, **1**, 26-29 (2017).
5) K. Kurt, K.Rode, M. Venkatesan, P. Stamenov and J. M. D. Coey: *Phys. Rev.* **B**, 83, 020405R (2011).
6) A. Sugihara, K. Z. Suzuki, T. Miyazaki and S. Mizukami: *J. Appl. Phys.*, **117**, 17B511 (2015).
7) H. Yoda, T. Kishi, T. Nagase, M. Yoshikawa, K. Nishiyama, E. Kitagawa, T. Daibou, M. Amano, N. Shimomura, S. Takahashi, T. Kai, M. Nakayama, H. Akikawa, S. Ikegawa, M. Nagamine, J. Ozeki, S. Mizukami, M. Oogane, Y. Ando, S. Yuasa, K. Yakushiji, H. Kubota, Y. Suzuki, Y. Nakatani, T. Miyazaki and K. Ando: *Curr. Appl. Phys.*, **10**, e87 (2010).
8) K. Z. Suzuki, R. Ranjbar, A. Sugihara, T. Miyazaki and S. Mizukami: *Jpn .J. Appl. Phys.*, **55**, 010305 (2016).
9) J. Wintelik, B. Bake, G. H. Fecher, M. C. M. Alves, F. Bernardi and J. Morais: *Phys. Rev.* **B**, 77, 054406 (2008).
10) S. Mizukami, F. Wu, A. Sakuma, J. Walowski, D. Watanabe, T. Kubota, X. Zhang, H. Naganuma, M. Oogane, Y. Ando and T. Miyazaki: *Phys. Rev. Lett.*, **106**, 117201 (2011).
11) M. Glas, D. Ebke, I. M. Imort, P. Thomas and G. Reiss: *J. Magn. Mater.*, **333**, 134 (2013).
12) M. Li, X. Jiang, M. G. Samant, C. Felser and S. S. P. Parkin: *Appl. Phys. Lett.*, **103**, 032410 (2013).
13) Y. Miura and M. Shirai: *IEEE Trans. Magn.*, **50**, 1400504 (2014).
14) J. W. Koo, S. Mitani, T. T. Sasaki, H. Sukegawa, Z. C. When, T. Ohkubo, T. Niizeki, K. Inomata and K. Hono: *Appl. Phys. Lett.*, **103**, 19241 (2013).
15) Y. Takahashi, K. Sato, T. Shima, and M. Doi: *AIP Adv.* **8**, 056315 (2018).
16) B. D. Schrag, A. Anguelounch, S. Ingvarsson, Gang Xiao, Yu Lu, P. L. Trouilloud, A. Gupata, R. A. wanner, W. J. Gallagher, P. M. Rice and S. S. P. Parkin: *Appl. Phys. Lett.*, **77**, 2373 (2000).
17) H. D. Chopra, D. X. Yang, P. J. Chen, D. C. Parks, and W. F. Egelhoff, Jr.: *Phys. Rev.* **B**, 61, 9642 (1999)
18) A. Koeba, T. Shima and M. Doi: *Jpn .J. Appl. Phys.*, **55**, 07MC04 (2016).

Received Oct. 13, 2017; Accepted June 14, 2018